CONF-860605--2

Gas-Bubble Growth Mechanisms in the Analysis of Metal Fuel Swelling*

by

E. E. Gruber and J. M. Kramer

CONF-860605--2

DE86 005512

ABSTRACT

During steady-state irradiation, swelling rates associated with growth of fission-gas bubbles in metallic fast reactor fuels may be expected to remain small. As a consequence, bubble-growth mechanisms are not a major consideration in modeling the steady-state fuel behavior, and it is usually adequate to consider the gas pressure to be in equilibrium with the external pressure and surface tension restraint. On transient time scales, however, various bubble-growth mechanisms become important components of the swelling rate. These mechanisms include growth by diffusion, for bubbles within grains and on grain boundaries; dislocation nucleation at the bubble surface, or "punchout"; and bubble growth by creep. Analyses of these mechanisms are presented and applied to provide information on the conditions and the relative time scales for which the various processes should dominate fuel swelling. The results are compared to a series of experiments in which the swelling of irradiated metal fuel was determined after annealing at various temperatures and pressures. The diffusive growth of bubbles on grain boundaries is concluded to be dominant in these experiments.

* This work was performed under the auspices of the US Department of Energy.

I. INTRODUCTION

There has recently been a renewed interest in using uranium-based metal alloys as a fuel for Liquid Metal Cooled Fast Reactors (LMRs). One of the most promising fuel types is an alloy of uranium, plutonium and zirconium [1]. As with all nuclear fuels, the behavior of gases generated by fission is of major concern in assessing the performance of metallic fuels during steady-state operation and during off-normal accident events.

A major effect of fission gas during off-normal transients lies in its influence on fuel motion. Negative reactivity, introduced when fuel is removed from the high worth region of the reactor core, has the potential to strongly reduce the energetic consequences of an unprotected accident. Even small amounts of fission gas can contribute significantly to fuel motion.

The effects of fission gas are of particular concern in analysis of the behavior of metal fuels. Current fuel design provides for significant radial swelling of metal fuels during steady-state irradiation. This feature permits the resulting porosity to interconnect, thereby promoting release of subsequently generated gas and preventing excessive cladding stresses [1]. Despite this release, a significant inventory of fission gas is retained in the porous fuel after relatively low burnup. During a thermal excursion, this trapped gas can provide a driving force for axial movement, or extrusion, of the fuel within the cladding. This extrusion would be significantly enhanced by the formation of a eutectic film at the fuel-cladding interface.

In order to evaluate the potential for extrusion, its rate, and its timing, it is necessary not only to specify the amount of gas available in the fuel, and its configuration, but also to characterize the time rate of response of the gas-bearing fuel to a transient situation. In the present work, alternate mechanisms of bubble growth are considered explicitly to determine which are applicable to the transient response of metal fuel. The results are discussed in relation to a series of experiments on irradiated metal fuel, subjected to heating under various pressures.

II. MECHANISMS OF BUBBLE GROWTH IN CRYSTALLINE SOLIDS

For heating rates and times of interest to accident analysis, fission-gas bubbles will generally not be in equilibrium with the external pressure. In this section we investigate the various mechanisms by which overpressured bubbles may grow in metal fuels.

A. Growth by Diffusion

Growth of fission gas bubbles by diffusion of vacancies, both within grains [2] and on grain boundaries [3], has been treated previously. The equations for bubble growth are: for bubbles within grains,

$$\frac{dr}{dt} = \frac{\Omega D_v \phi}{rkT[1 + d_g(\pi N\bar{r})^{1/2}/3]} ; \tag{1}$$

and for bubbles on grain boundaries,

$$\frac{dr}{dt} = \frac{\Omega D_{gb} w \sin^3 \theta}{2kTr^2 Ln} \phi . \tag{2}$$

In these equations, r represents the bubble radius (the radius in the grain boundary for Eq. 2); t is time; D_v is the volume-diffusion coefficient; $D_{gb}w$ is the product of the grain-boundary diffusion coefficient and the boundary thickness; Ω is the atomic (or molecular) volume; kT is the thermal energy; and ϕ is the overpressure, defined by

$$\phi = P_g - P_x - 2\gamma/\rho. \tag{3}$$

This overpressure represents the excess of gas pressure P_g over the sum of the external hydrostatic pressure P_x and the surface-tension restraint, defined in terms of the surface tension (more accurately, the specific surface free energy) γ and the radius of curvature ρ. For bubbles within the grains, ρ is simply the radius r; for grain-boundary bubbles, $\rho = r/\sin\theta$, where θ is the intersection angle between the bubble surface and the grain boundary. Geometric considerations are involved in Eq. 2 in the parameters

$$\eta = 1.0 - 0.5 \cos\theta(3 - \cos^2\theta),$$

which enters the relationship for the volume of the lenticular bubble, and

$$L = \alpha - [3 + \alpha^2 + \ln(\alpha^2)]/4,$$

which characterizes the effect of bubble spacing in the boundary. Here,

$$\alpha = (r/\ell)^2,$$

with ℓ the spacing, or "cell radius", in the boundary.

Finally, the term in brackets in the denominator of Eq. 1 represents the vacancy-depletion effect, modeled after Wood et al. [4]. The grain diameter d_g is used to characterize the migration distance for vacancies, and extension of the analysis to a distribution of bubble sizes is accomplished by the use of the mean bubble radius $\bar{r}$ and the number of bubbles per unit volume of fuel, N.

B. Growth by Dislocation Nucleation

The possibility that an overpressured bubble can expand by generating a dislocation loop has been considered in the past. Greenwood calculated the required overpressure to generate such a loop by considering the bubble as a Frank-Read source; his result is [5]

$$P_g > (2\gamma + \mu b)/r. \qquad (4)$$

where μ is the shear modulus and b is the Burgers vector. We consider here a more direct derivation, based on consideration of the change in free energy when a "pillbox" of radius r' is formed by nucleating a dislocation loop of the same radius. The free energy change is given by

$$\Delta G = 2\pi r'(\mu b^2 + \gamma b) - (P_x - P_g)\,\pi r'^2 b.$$

In this equation, μb^2 is the approximate energy per unit length of dislocation, γb is the surface energy per unit length of ledge, and the volume term represents the work done against the external pressure and that gained by expansion of the gas within the bubble.

Specifying a free-energy change less than zero for spontaneous nucleation of a dislocation loop, the result simplifies to

$$P_g - P_x > 2(\mu b + \gamma)/r'.$$

The right hand side of this relation is a minimum when r' is a maximum, or r' = r; the critical overpressure is therefore given by

$$P_g - P_x - 2\gamma/r \equiv \phi^* = 2\mu b/r. \qquad (5)$$

This result is somewhat more general and more accurate than the Greenwood approximation. It also leads to the conclusion that a sufficiently overpressured bubble of radius r will "punch out" a dislocation loop of the same radius r, in a diametral plane. (A similar process is discussed by Friedel [6]; if an indenter is pressed against the surface of a crystal, an indent is created by introducing loops of "prismatic" edge dislocations.) Once nucleated, these dislocation loops are free to move away from the bubble by glide. A dramatic illustration is provided by Friedel in his Fig. 1.25, which shows punching of dislocations around glass spheres in AgCl, as observed by Jones and Mitchell [7]. This illustration further demonstrates that the loop radius is the same as the sphere radius.

It should be noted that once nucleated, the prismatic dislocation loop is equivalent to the edge of an extra plane of atoms inserted in the lattice. Such a loop should provide an efficient sink for atoms (or equivalently a source for vacancies) that will allow the associated overpressured bubble to expand by relatively short-range diffusion. This process is coupled to radial expansion of the loop, or "climb". On the other hand, if a number of loops should be formed successively, they would repel, moving away from the bubble by glide. As a result, any loops punched out will move away from the bubble, either by climb or by glide. This behavior makes it unlikely that the

bubble would intersect dislocations generated by its own overpressure, as has been conjectured in some arguments on bubble mobility [8].

Taking some estimated values of the material parameters for metal fuel, the critical overpressure for dislocation punch-out is

$$\phi^* = 2\mu b/r = 2(5\times10^4 \text{ MPa})\ (0.275\text{nm})/r$$
$$= 2.75 \times 10^4/r \text{ MPa}$$

for r in nm. This value exceeds the surface-tension restraint $2\gamma/r$ by a factor of about 14. Dislocation punchout should therefore occur only for severely overpressured bubbles. (For oxide fuel, both μ and γ are reduced, but the ratio of critical overpressure to surface-tension restraint is still about 14.)

C. Growth by Creep

Bubbles may also grow by creep through climb and glide of existing dislocations. This mechanism of swelling in metal fuels has also recently been considered by Miles and Kalimullah [9]. The bubble radius r is calculated using the classical solution[1] for creep growth of a spherical cavity under pressure. Using the previously defined notation the growth rate is given by

$$\frac{dr}{dt} = \frac{Br}{2}\left[\frac{3\phi}{2n\left[1 - \left(\frac{r}{r_c}\right)^{3/n}\right]}\right]^n \qquad (6)$$

where ϕ is the overpressure and r_c is the bubble cell radius, defined by $r_c^3 = \frac{3}{4\pi N}$. The parameters B and n are determined from the fuel creep law which is assumed to be of the power law form

---

[1] The usual reference for this result is Finnie and Heller [10, p. 187]. It should be noted, however, that there are several typographical errors in their equations. The equations for creep growth of a sphere are rederived correctly in Ref. [9].

$$\dot{\bar{\varepsilon}} = B\bar{\sigma}^{n} \tag{7}$$

where $\dot{\bar{\varepsilon}}$ is the equivalent strain rate and $\bar{\sigma}$ is the equivalent stress.

The creep equation for metal fuels used here is the correlation for secondary creep developed by Kramer [9]. In the low temperature regime where creep is dominated by the deformation of the α uranium matrix the creep rate is given by

$$\dot{\bar{\varepsilon}} = (0.5 \times 10^{4}\,\bar{\sigma} + 6.0\bar{\sigma}^{4.5}) \exp(-26{,}170/T)\ s^{-1} \tag{8}$$

where $\bar{\sigma}$ is in MPa. At higher temperatures where the γ solid solution phase is formed the creep rate is given by

$$\dot{\bar{\varepsilon}} = 8.0 \times 10^{-2}\,\bar{\sigma}^{3} \exp(-14{,}350/T)\ s^{-1}. \tag{9}$$

It should be noted that the activation energies for creep in these two regimes are close to the activation energies for volume diffusion, as would be expected from theory. It is also noted that Eq. 8 is the sum of two terms of the form of Eq. 7. We will superimpose the bubble growth rate given by using each term separately in Eq. 6. This approach is not strictly valid because the creep equation is non-linear. However, the error incurred is probably small because one term or the other tends to dominate the creep rate depending on the magnitude of the stress.

Growth of grain boundary bubbles by creep of the surrounding matrix is also considered. The critical dimension governing the creep rate of these bubbles is assumed to be the thickness of the tendon separating each bubble on the boundaries. The bubble geometry is therefore modeled as a cylinder with an inner radius equal to the radius of the bubble footprint r and an outer radius equal to the cell radius ℓ, as defined in connection with Eq. 2. The growth rate of the radius of the cylinder is given by [10, p. 184]

$$\frac{dr}{dt} = B\left(\frac{3}{4}\right)^{\frac{n+1}{2}} r\left[\frac{2\phi}{n\left[1 - \left(\frac{r}{\ell}\right)^{2/n}\right]}\right]^{n} \tag{10}$$

The increase in length due to creep is zero.

The applicability of the above creep analysis to the growth of fission gas bubbles in metal fuels requires some comment, although the equations will be applied in the following section without regard to their validity. First, since matrix creep is assumed it may be questioned whether or not the linear creep term in Eq. 8 should be included, since it often represents creep by diffusion to grain boundaries under tension. If this is the case a definite grain size dependence of the constant B would be expected. Although there is some suggestion of such a dependence, the evidence from the available creep data is not clear. A linear stress dependence could also indicate Harper-Dorn dislocation creep of the matrix.

The second restriction on the validity of the creep analysis is more severe. It would not be appropriate to assume bubbles can grow by creep of the surrounding matrix if the size of the bubbles were much smaller than the spacing of the dislocations. The dislocation density in metals might be expected to range from $10^{12}/m^2$ for well-annealed material to $10^{16}/m^2$ for heavily worked material. The corresponding dislocation spacing is 10^{-6} to 10^{-8} m. Overpressures in very small bubbles are therefore not likely to create stress fields that move existing dislocations.

It has also been suggested that primary creep may allow bubbles to grow faster than calculated by using Eqs. 6 and 10, where only secondary creep is considered. Indeed, for many materials primary creep rates are an order of magnitude greater than secondary creep rates. However, solid solution alloys, such as the high temperature γ phase of metal fuels where creep is most important, often show the opposite type of primary creep behavior where the creep rate increases with increasing strain. These alloys have been termed Class I solid solution alloys [11]. Creep is limited by solute drag yielding a power law exponent of 3 as was found in the correlation given by Eq. 9. Furthermore, creep data for γ U-Zr alloys [12] at 815 and 982°C show this type of behavior where the primary creep rate is lower than the secondary creep rate.

Even if the primary creep rates are high, they probably would not contribute significantly to the equilibration of matrix fission gas bubbles

because primary creep strains are typically several percent at most. Much larger creep strains are necessary to equilibrate small bubbles, as can be seen by relating the tangential strain ε_t at the bubble surface to the swelling $\Delta V/V$. Since the material surrounding the bubbles may be assumed incompressible, ε_t can easily be shown to equal

$$\varepsilon_t = \frac{\Delta r}{r_o} = \frac{1}{3}\frac{\Delta V}{V} / \left(\frac{r_o}{r_{co}}\right)^3$$

where r_o and r_{co} are the initial bubble radius and cell radius, respectively. The cubic term is just the initial bubble porosity. In most cases the bubble porosity is only a few percent, thus requiring strains at the bubble surface one or two orders of magnitude greater than the swelling.

D. Comparison of Swelling Rates by Alternate Bubble-Growth Mechanisms

A series of calculations has been carried out to isolate the swelling contributions of the various bubble-growth mechanisms, and to determine the dominant mechanisms for different transient conditions. These calculations were accomplished by means of a simple interactive FORTRAN program, called BUBBEX (for BUBBle EXpansion). The code accepts initial and transient conditions, and calculates the consequent bubble growth as a function of time.

The initial values of burnup, temperature, pressure, bubble size, and grain size are used to establish an equilibrium starting condition. All of the gas associated with the given burnup is presumed present in bubbles of the initial size, with the gas pressure in equilibrium with the external pressure and temperature. The modified van der Waals gas law is used to calculate the number of gas atoms per bubble; the total number of bubbles per unit initial volume is then determined from the burnup; and the fuel volume per bubble is used to define a cell radius r_c.

A separate version of the code was developed to treat lenticular grain-boundary bubbles. The grain-boundary area per unit volume is calculated from the grain size. Again, the burnup and initial bubble size, temperature, and pressure are used to calculate the number of atoms per bubble, bubble density, and cell radius in the boundary. This cell radius is used to deter-

mine the parameter L in Eq. 2, and is used in the grain-boundary creep calculation represented by Eq. 10.

The temperature and/or pressure is then changed to a new value, and the code calculates the consequent bubble growth and swelling as functions of time. The BUBBEX code was programmed to accept an alternate option if the final temperature and pressure are both the same as the initial values: the bubbles are all assumed to combine pairwise at constant volume. The subsequent expansion of these overpressured product bubbles is then calculated. The four separate growth relations, represented by Eqns. 1, 2, 6, and 10, were applied in the BUBBEX code. The term in brackets in Eq. 1, representing vacancy-depletion effects, was not used in these calculations. The results thus represent an upper limit to swelling by volume-diffusion growth of matrix bubbles. For a grain size of 1 μm (mean linear intercept) and conditions typical of the examples given in this section, vacancy depletion reduces the bubble growth rate by about a factor of two.

Dislocation punchout was also not considered in this comparison, since it is ideally not a time-dependent process. Further, an overpressure of 27.5MPa, or about 4000psi, would be required for dislocation nucleation for a bubble of 1 μm radius. For bubbles one-tenth as large, typical of most of the examples used here, the critical overpressure would be ten times as large.

The swelling rate is characterized in the following by the "equilibration time" τ, which is defined by approximating the bubble growth as an exponential, in the form

$$r = r_o + (r_{eq} - r_o)(1 - e^{-t/\tau}). \qquad (11)$$

The value of τ is determined from the initial rate of bubble growth. Differentiating Eq. 11 and solving for τ at time t=0 gives

$$\tau = (r_{eq} - r_o)/(dr/dt)_{t=0}. \qquad (12)$$

The exponential approximation is often quite accurate, even though not strictly valid. However, high accuracy is not necessary in our application. The

exponential approximation is still useful because it provides a means of comparing initial swelling rates by various mechanisms, and it provides a more efficient method of performing the finite-difference calculations. When linear forward-difference calculations are used, oscillations often develop in the calculated results when bubbles approach the equilibrium size. The internally calculated time steps then become quite small, and the calculation becomes inefficient. The use of the formalism represented by Eq. 11 permits excellent accuracy with fairly large time steps. [3]

To simplify the BUBBEX calculations, the activation energies for diffusion and creep were taken to be the same, and equal to the values described for creep in the previous section. The diffusion coefficient for the α phase was taken to be 10^{-18} m^2/s at 640C [13], so that $D_0 = 2.8X10^{-6}$ m^2/s. The transition to the γ phase is assumed to occur at 650C for U-5%Fs fuel; the β phase is not considered in this analysis. The pre-exponent for diffusion in the γ phase is taken to be $2.33X10^{-7}$ m^2/s, which corresponds in the Boltax tabulation [13] to the activation energy used here.

Figure 1 shows the results of a series of calculations carried out with the BUBBEX code to determine the dependence of the time constant τ on temperature for the various mechanisms. In all of these calculations, bubbles of initial radius r=100nm, in equilibrium with an external pressure of 0.7MPa (100psi), are assumed to combine in pairs to form overpressured bubbles. The bubble density is calculated from the gas generated during the assumed 1 atom percent burnup of the fuel. The grain size[1] is assumed to be 1 μm. The time constants increase uniformly as the mechanism for bubble growth changes from grain-boundary diffusion, to bulk diffusion, to grain-boundary creep, to creep. Except for the grain-boundary diffusion growth, in which the diffusion coefficient is assumed to change continuously, there is a significant decrease in the time constant when the temperature enters the γ range.

---

[1] The grain size as used here is assumed to be the size of grains within a single phase, measured by the mean linear intercept method. More generally, grain size refers to the effective size determined by the spacing of any internal surfaces that might trap bubbles. These surfaces may be interphase boundaries or interfaces between precipitates and the fuel material, as well as boundaries within a single phase.

The dependence of the swelling rate on bubble size differs for the different mechanisms. A series of calculations was completed to show the dependence on bubble size at 800C for the same burnup, pressure, and grain size as considered above. The results, shown in Fig. 2, show that grain-boundary diffusion still dominates up to about 300nm bubbles, at which point the time constants are becoming fairly large.

The results of a similar series of calculations is shown in Fig. 3; in this case, a constant overpressure ϕ = 33.8MPa is used, by reducing the pressure from 34.5MPa (5000psi) to 0.7Mpa (100psi). This modification has the effect of decreasing the time constant for creep growth of large bubbles significantly, in comparison to the previous calculations. The difference arises because pairwise coalescence leads to much lower overpressures for the larger bubbles; creep is more sensitive to stress than the diffusive growth mechanisms, since the stress exponent is 3 for creep in the γ phase.

A wide variety of conditions could be considered in comparing relative values of the swelling time constant. The results are sensitive to all the parameters of interest. The two criteria used in obtaining the results shown in Figs. 1 through 3 are diverse enough, however, to develop some general conclusions. It appears that grain-boundary diffusion will dominate creep for bubbles on grain boundaries, and that diffusive growth will be faster than creep for bubbles within grains.

In considering swelling as a consequence of only bubble growth (without coalescence), the initial bubble size is an important factor. If the bubbles are very small, even if highly overpressured, the swelling associated with their growth to equilibrium size is very small. The potential swelling associated with the results shown in Fig. 3 is shown as a function of initial bubble radius in Fig. 4. If the fission gas bubbles are characterized by a mean bubble radius, it is apparent that that radius must be on the order of 100nm for significant swelling to occur.

This relationship has been applied to establish initial conditions for analysis of a series of transient swelling experiments on Mark-II fuel after 0.8 at.% burnup [14]. Specimens were induction heated under hydrostatic

pressure of 34.5MPa and held at various temperatures. The pressure was then reduced to 0.7MPa, and swelling was determined at various times by immersion density measurements. With the assumption that the initial bubble radius is 100nm, calculations were carried out to determine the swelling as a function of time for two of the experimental temperatures.

The results for the different growth mechanisms are shown in Fig. 5. Swelling ranged between limits of about 2% and 7%, depending somewhat on the temperature, and on whether the bubbles were assumed in the grains or on grain boundaries. Initial and final equilibrium values of swelling for the different conditions are indicated by the horizontal series of symbols. The times required for swelling to occur by bulk diffusion or by either type of creep are quite long --- greater than 10^5s. It must be concluded that if swelling results only by bubble growth, as proposed by the experimenters, diffusive growth of grain-boundary bubbles is the only acceptable mechanism.

Discrepancies remain between the experimental and calculated results, however. The measured swelling changes (relative to the initial swelled state) at 100s were about .6% at 550C, and 3.5% at 600C. The calculated total swelling at 100s is 4% at 550C, and 6% at 600C. Subtracting the initial swelling of 2.2 and 2.3%, the calculated swelling changes are 1.8 and 3.7%. This is excellent agreement for the 600C test, but the difference at 550C indicates that temperature alone does not explain the different swelling curves observed by the experimenters.

One possibility that should be expected is that the initial bubble size depends on the temperature; another is that some of the gas may not be on grain boundaries. Obviously, a wide range of "fitting" parameters is opened up. Fig. 6 shows one possible combination of parameters. For each temperature, the upper curve shows the total swelling, the dashed curve shows the observed swelling change, and the lower curve shows the calculated swelling change. The same parameters used above were used for the 600C calculations, with grain size of 1 μm, burnup of .8 at.%, and initial bubble radius of 100nm. For the 550C test, the initial bubble radius was reduced to 70nm, and the amount of gas on grain boundaries was reduced to 40% of the previous value by using a burnup of 0.32 at.%.

Even with these modifications, the swelling is calculated to change more rapidly than observed in these experiments. It is concluded that modeling swelling only in terms of expansion of bubbles of one size imposes a limitation on the accuracy of the results.

III. CONCLUSION

The considerations of the previous section lead to the conclusion that transient swelling of metal fuels can be approximated with some simple models, but that accurate characterization requires knowledge of a number of variables. These include the grain size, mean bubble size, and partitioning of bubbles in grains, on grain boundaries, and in edge porosity.

The calculations generally support the observed dependence of swelling on pressure. The agreement in time scales and swelling magnitude, from a comparison of growth rates by various mechanisms, supports the conclusion that diffusive growth of grain-boundary bubbles dominates the swelling rate.

The presence of internal surfaces, whether between grains of a single phase or between different phases, is important to both fuel swelling and fission-gas release kinetics. The effective grain size at operating conditions is therefore a parameter that should be well characterized for realistic analysis of fuel behavior. The tendency for bubbles to collect on these internal surfaces enhances the swelling rate for small bubbles, and leads to early interconnection of porosity, with associated release of gas from the fuel.

In general, accurate modeling of transient swelling must consider a variety of effects, in addition to the growth of average bubbles. The FRAS3 code [15] models the most important of these effects, including migrational coalescence, transfer of bubbles to grain boundaries, the kinetics of bubble growth, and development of edge porosity. This code is operational with optional parameters for metal fuel. It is recognized that simplified models are needed for applications where such detailed modeling is inappropriate. However, development of such models should rely on the more detailed results to establish appropriate simplifying assumptions, acceptable approximations, and ranges of applicability.

References

1. L. C. Walters, B. R. Seidel, and J. H. Kittel, "Performance of Metallic Fuels and Blankets lin Liquid-Metal Fast Breeder Reactors", Nucl. Tech. 65 (May 1984), pp. 179-231.

2. E. E. Gruber, "The Role of Bubble-Size Equilibration in the Transient Behavior of Fission Gas," USDOE Report ANL-78-36 (April 1978).

3. E. E. Gruber, "Diffusional Growth of Overpressured Fission-Gas Bubbles on Grain Boundaries," J. Nucl. Mat. 110 (1982), pp. 223-229.

4. M. H. Wood, J. R. Matthews, and H. R. Matthews, "Comparison of Experiment and NEFIG Model Calculations of Transient Fission Gas Behavior", J. Nucl. Mat. 87 (1979), pp. 167-174.

5. G. W. Greenwood, A.J.E. Foreman, and D. E. Rimmer, "The Role of Vacancies and Dislocations in the Nucleation and Growth of Gas Bubbles in Irradiated Fissile Material," J. Nucl. Mat. 1 (4) (1959), pp. 305-324.

6. J. Friedel, "Dislocations", Pergamon Press (New York, 1964), p. 230.

7. D. A. Jones, and J. W. Mitchell, Phil. Mag. 3 (1958), p. 334.

8. J. Rest, and S. M. Gehl, Trans. Am. Nucl. Soc., Vol. 28 (June 1978), p. 239.

9. K. J. Miles and Kalimullah, "The Inherent Safety Phenomenon of Fission-gas Induced Axial Extrusion in Oxide and Metal Fueled LMFBR's" to be published in the Proceedings of the International Topical Meeting on Fast Reactor Safety, Knoxville, TN, April 21-25, 1985.

10. I. Finnie and W. R. Heller, Creep of Engineering Materials, McGraw-Hill (New York, 1959).

11. O. D. Sherby and P. M. Burke, "Mechanical Behavior of Crystalline Solids at Elevated Temperature," in Progress in Materials Science, Vol. 13, Pergamon Press, New York, 1967, pp. 325-90.

12. H. A. Saller et al., "Creep Strength of Uranium Alloys at 1500 and 1600F," BMI-834, May 28, 1953.

13. A. Boltax, in "Nuclear Reactor Fuel Elements, Metallurgy and Fabrication", ed. A. R. Kaufmann, Interscience (New York, 1962), p. 296.

14. J. A. Buzzell et al., "Transient Performance of EBR-II Driver Fuel," Proc. ANS/ENS Topical Meeting on Reactor Safety Aspects of Fuel Behavior (Aug. 2-9, 1981), Sun Valley, ID, p. 1-420.

15. E. E. Gruber, "Analysis of Transient Fission-Gas Release and Swelling in Oxide Fuel," Ceramic Advances (in press).

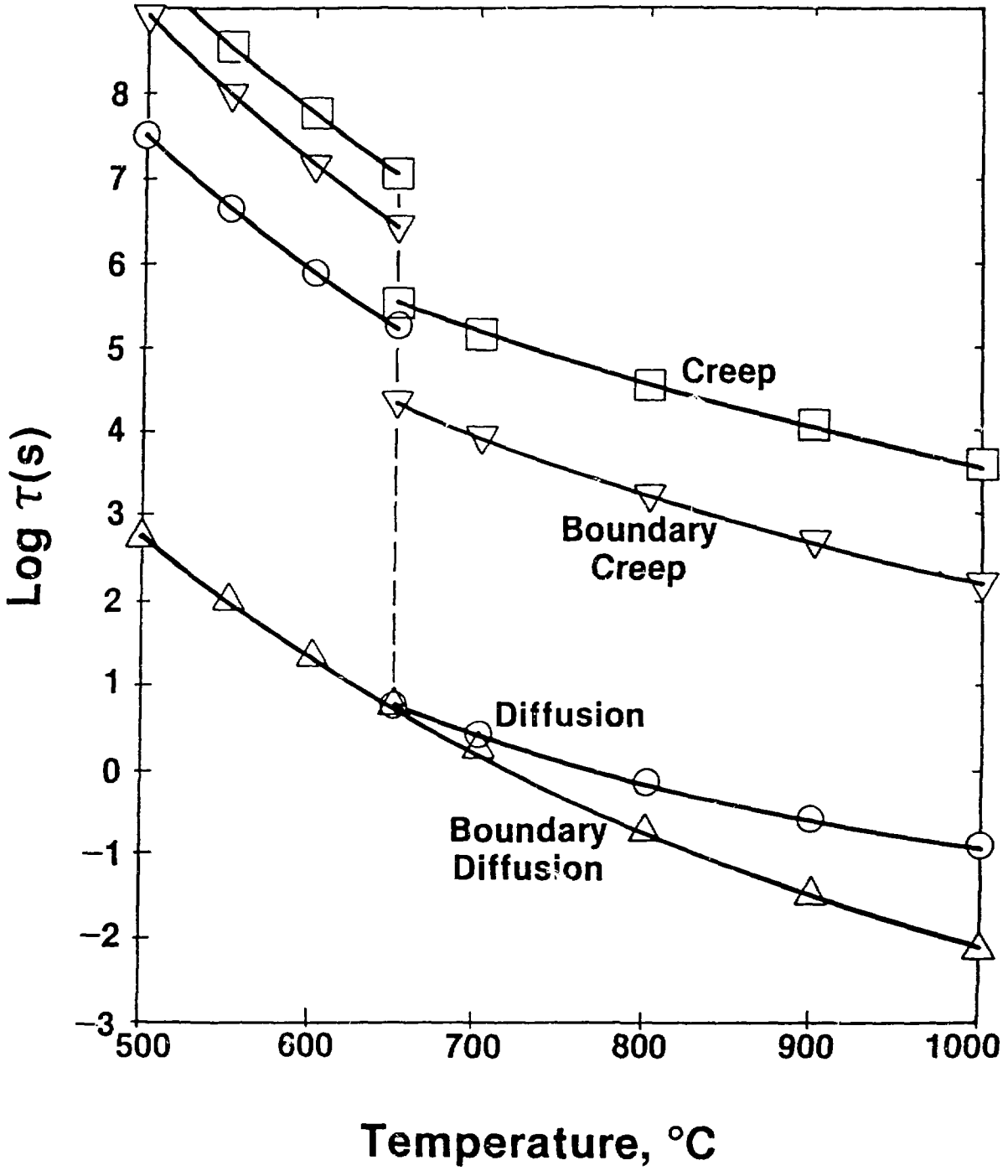

Fig. 1. Dependence of the bubble-growth time constant for pairwise coalescence of 100nm-radius bubbles on temperature.

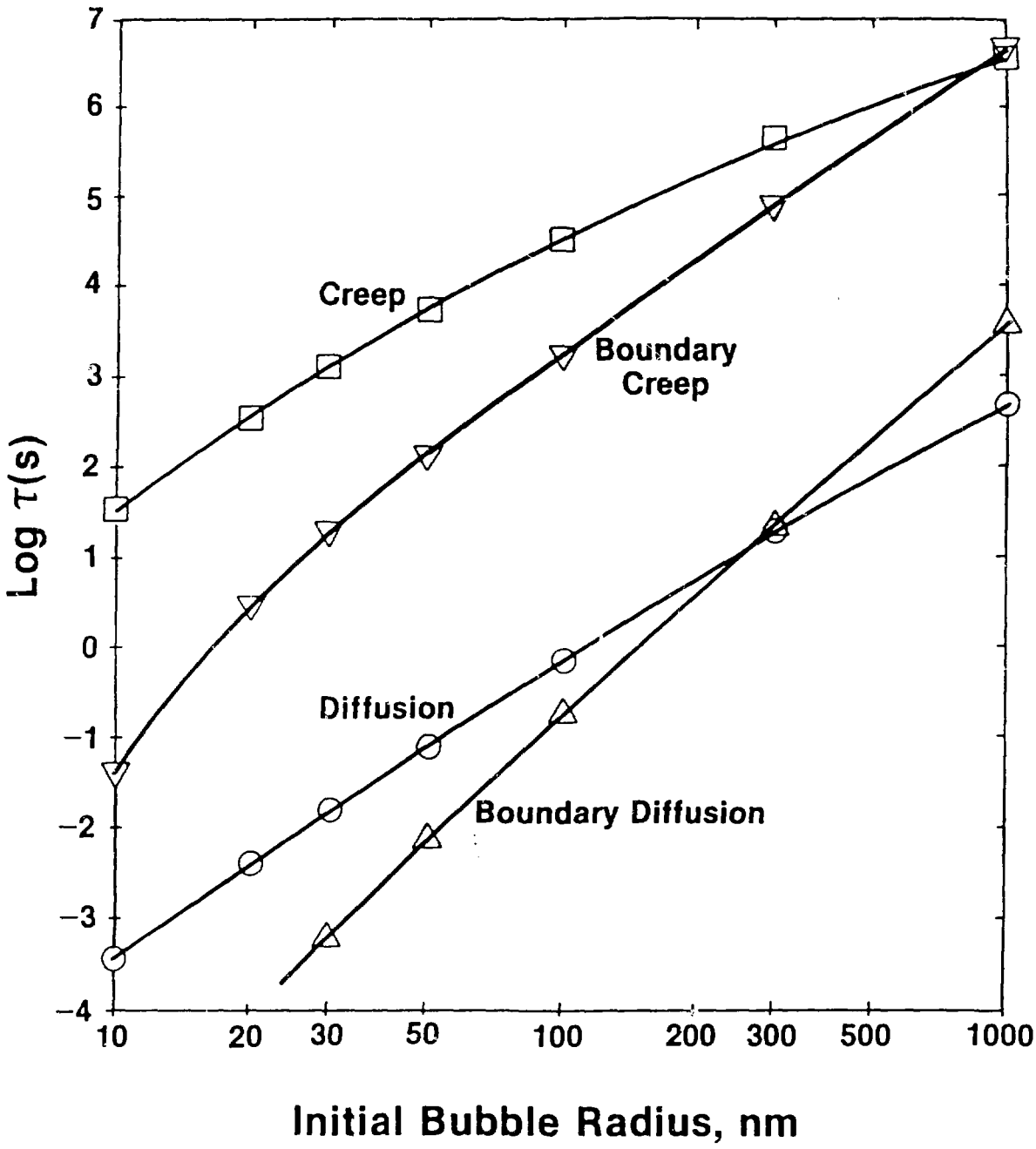

Fig. 2. Dependence of the bubble-growth time constant, for pairwise coalescence at 800C, on the initial bubble radius.

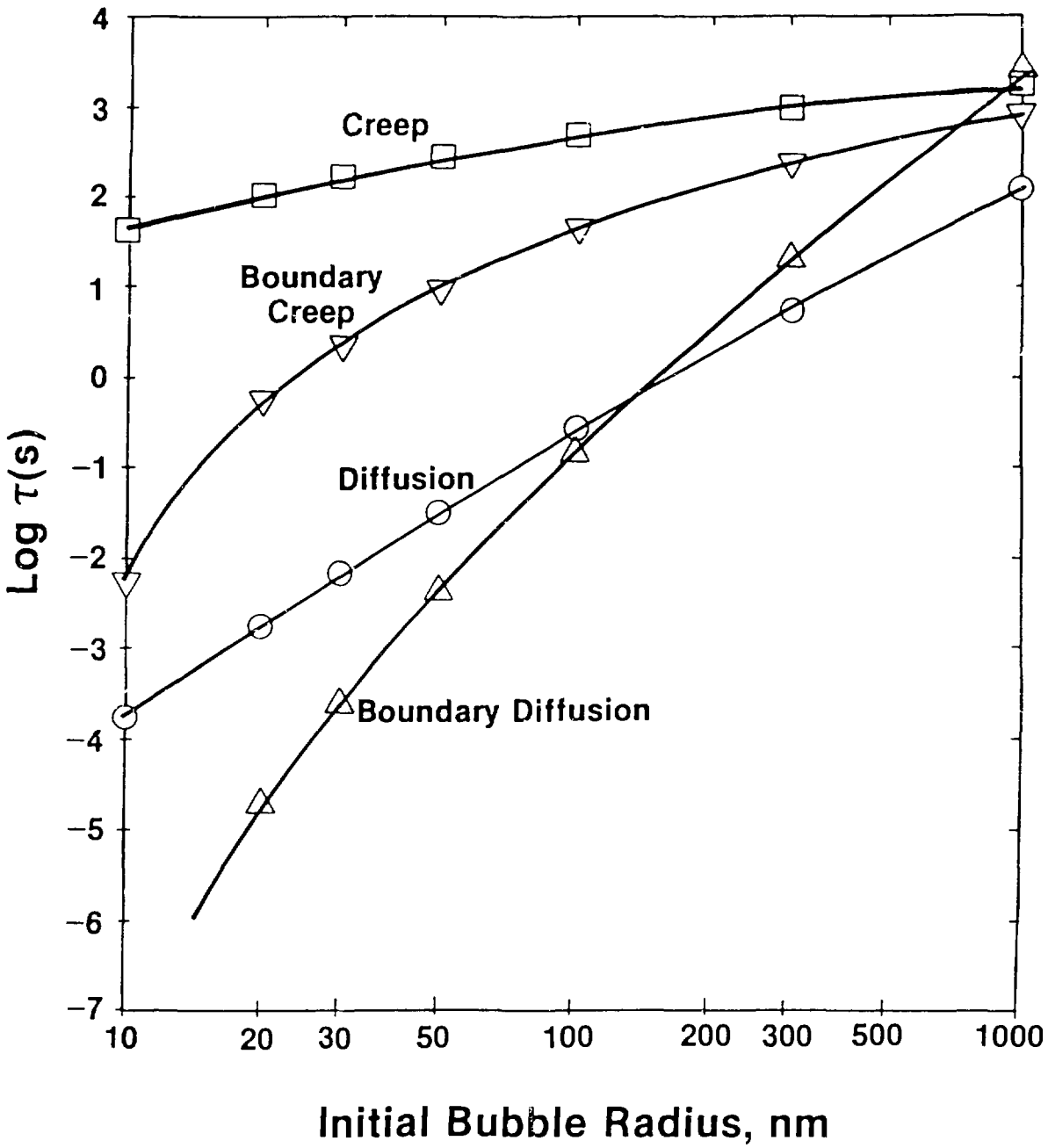

Fig. 3. Dependence of the bubble-growth time constant, for constant overpressure of 33.8MPa at 800, on the initial bubble radius.

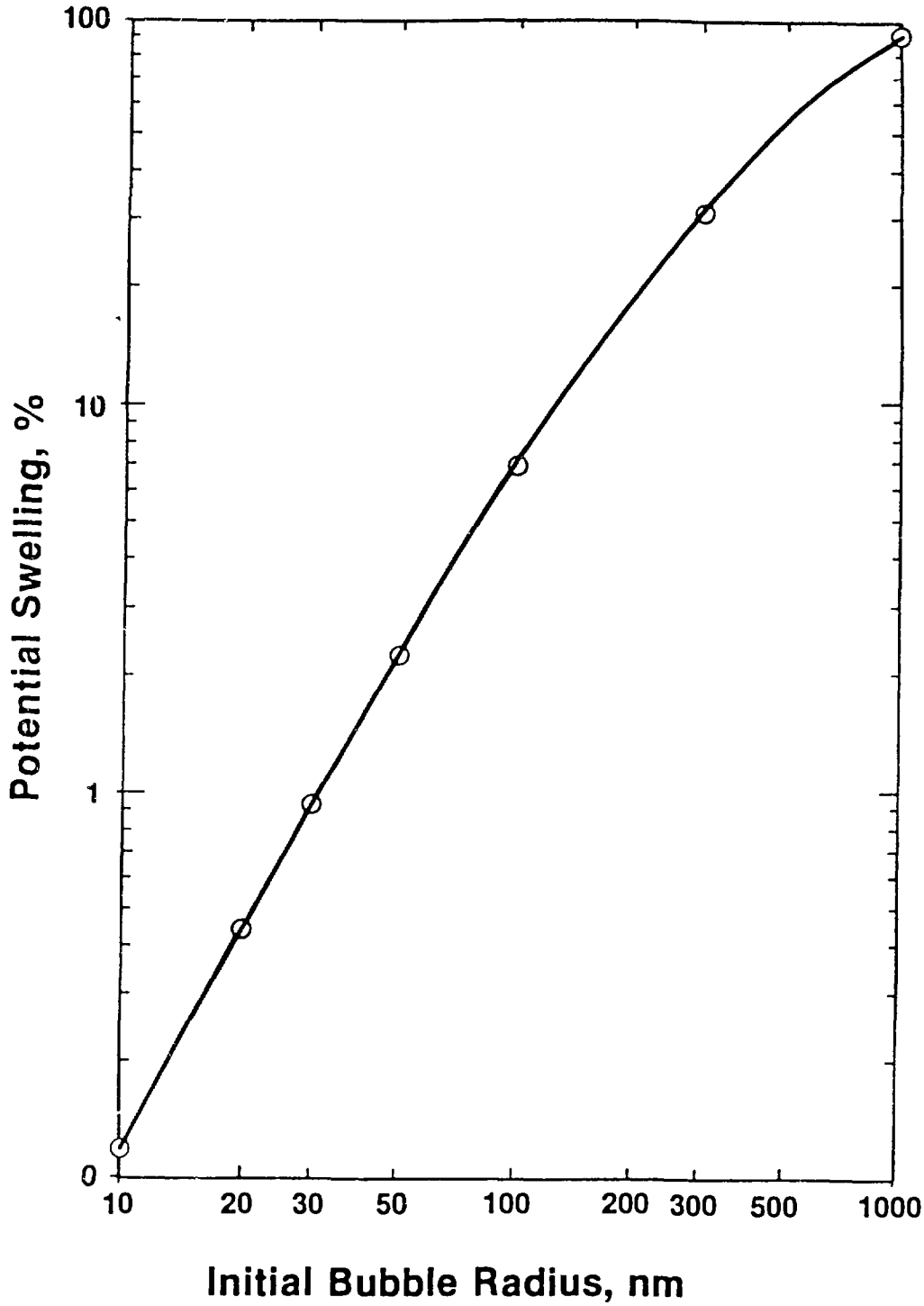

Fig. 4. Extent of potential swelling as a function of initial bubble radius for 1 at.% burnup, at initial overpressure of 33.8MPa and temperature of 800C.

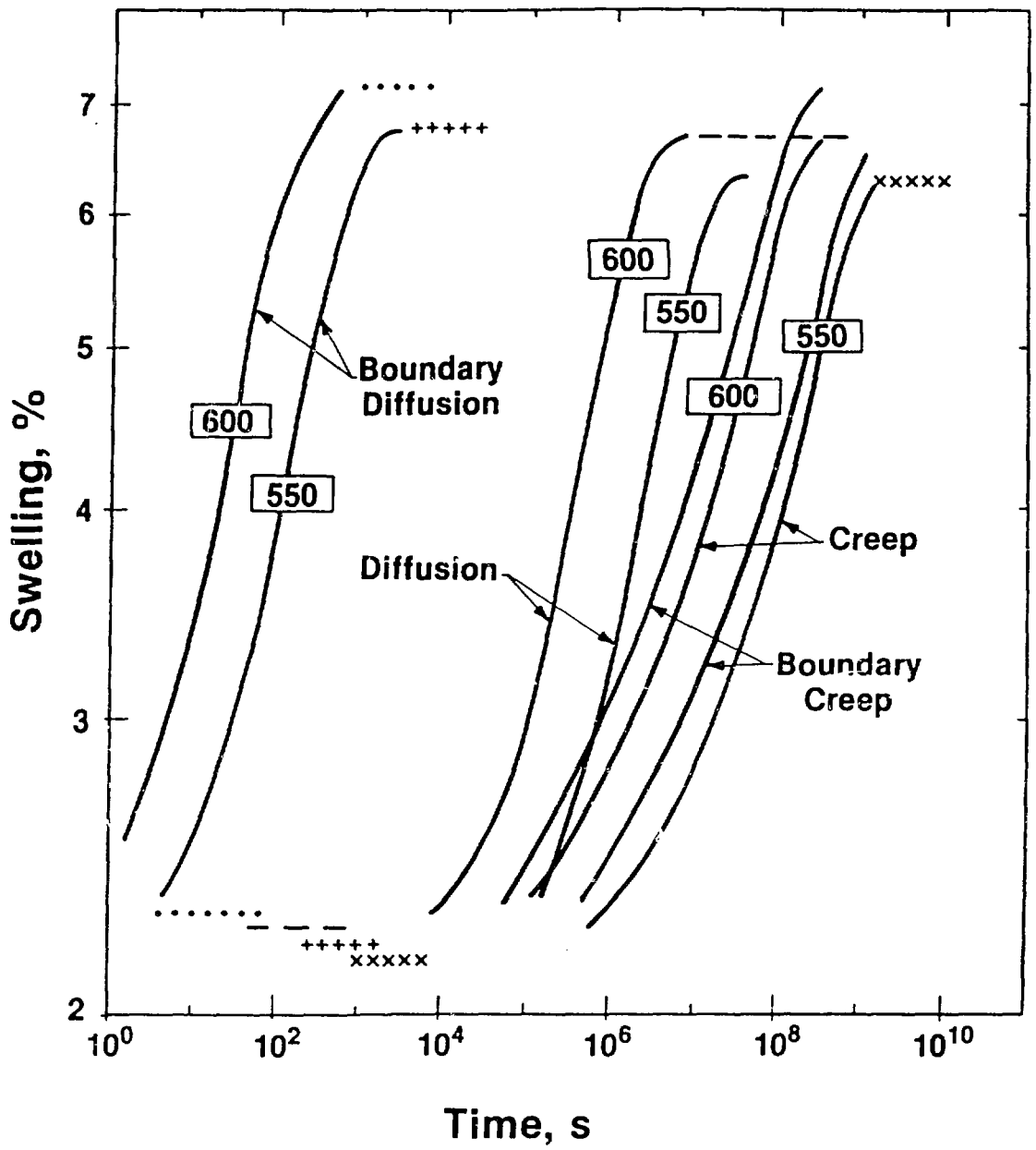

Fig. 5. Calculated dependence of fuel swelling on time, at 550C and 600C, for the four mechanisms considered independently.

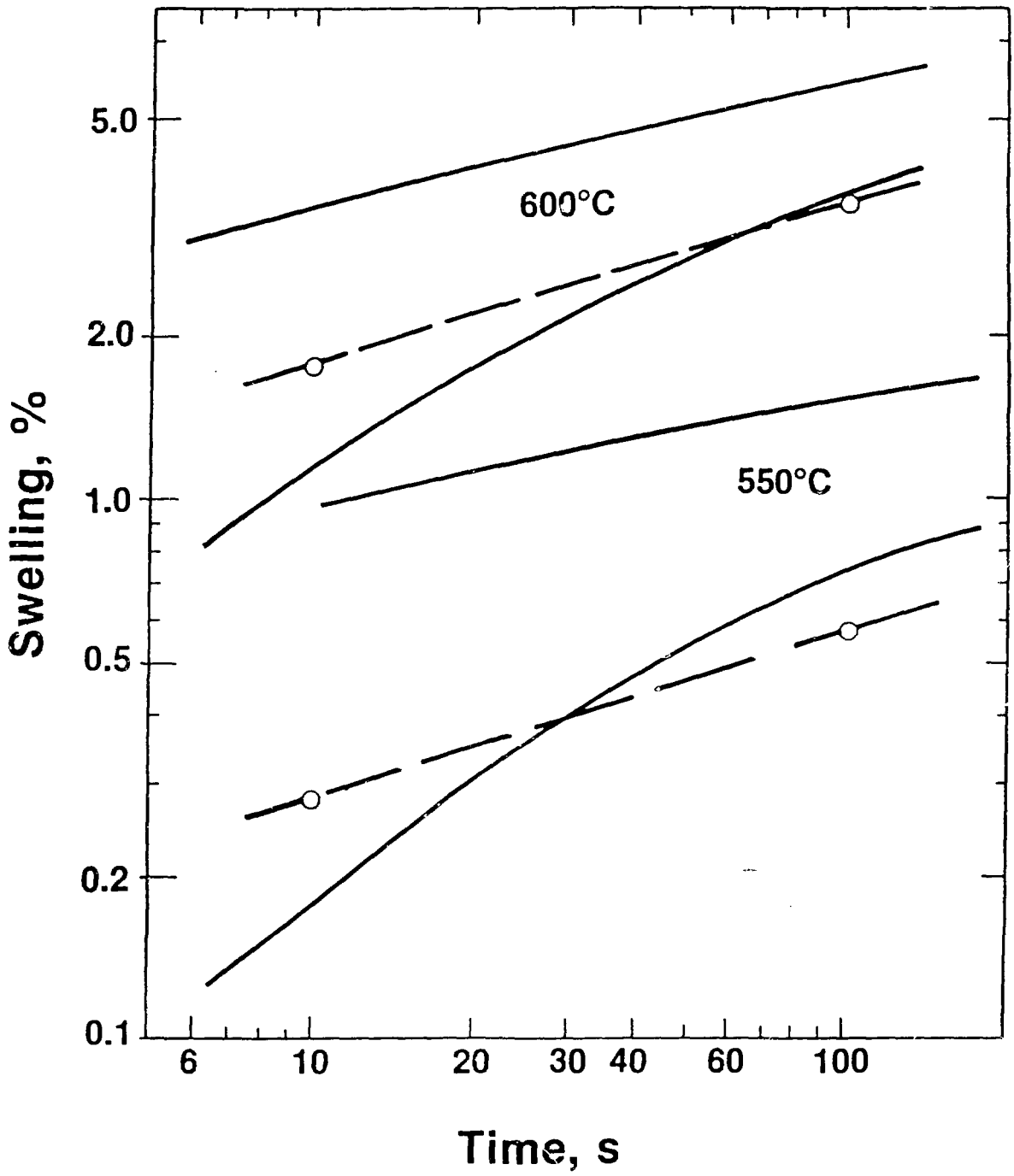

Fig. 6. Comparison of measured swelling (dashed lines) to calculated results (solid lines) at 550C and 600C. Upper solid line for each temperature indicates total swelling; lower one shows the swelling change from the initial value.